Travelling waves and static structures in a two-dimensional exactly solvable reaction-diffusion system

1999 J. Phys. A: Math. Gen. 32 8033

(http://iopscience.iop.org/0305-4470/32/46/304)

J. Phys. A: Math. Gen. **32** (1999) 8033–8044. Printed in the UK PII: S0305-4470(99)05634-6

Travelling waves and static structures in a two-dimensional exactly solvable reaction–diffusion system

Pavel K Brazhnik and John J Tyson

Department of Biology, Virginia Polytechnic Institute and State University, Blacksburg, VA 24061, USA

Received 1 July 1999

Abstract. Exact travelling wave solutions of a Fisher-type reaction–diffusion equation in two spatial dimensions are obtained. The waves have nontrivial geometries and possess velocities smaller and larger than that of a plane wave. The dispersion relationship and velocity-curvature dependence generated by these solutions are characterized. Static structures with and without circular symmetry are constructed.

1. Introduction

Finding solutions of nonlinear models is a difficult and challenging task. Several analytical methods have been developed for obtaining travelling wave solutions for pure dispersive nonlinear systems in one spatial dimension: the inverse scattering transfer [1], the Hirota method [2], Lamb's ansatz [3], etc [4]. Some of these methods may be extended to two-dimensional (2D) systems. The problem of obtaining solutions for systems including dissipative losses, e.g. reaction–diffusion systems, turned out to be more complex. Even for the 1D case, most of the above-mentioned methods do not work. These problems are usually treated by perturbation theory or numerical investigation [5–7]. Therefore, models of dissipative systems that admit exact solutions are indispensable for understanding possible behaviour in such systems.

The formal solution of some 1D reaction–diffusion models (e.g. quadratic Fisher equation) yields multiple travelling wave states. Furthermore, in two and three dimensions, the shape of the wavefront may change in the process of propagation and evolve to some stationary configuration (pattern) which is not necessarily trivial or unique. Therefore, a challenging problem in the theory of dissipative systems (which we partially address here) concerns the questions: what velocity and shape of the wave will develop in the evolution process and what is the selection mechanism? This nonequilibrium problem shares a common ground with physical kinetics, chemical reactions and living phenomena [8, 9].

In this paper we consider an autonomous Fisher-type equation with quadratic nonlinearity and modified diffusion

$$\phi_t - \Delta\phi - \frac{m}{1-\phi}(\nabla\phi)^2 = \phi(1-\phi). \qquad (1)$$

Here $\phi(t, x, y)$ is some kinetic variable, ∇ and Δ are gradient and Laplacian operators, respectively. For $m = 0$, equation (1) is the classical Fisher equation, which occurs in models of population growth [9], flame propagation [8], neurophysiology [10], autocatalytic chemical reactions [11], Brownian motion [12] and nuclear reactors [13]. The case $m = 2$ turns out to allow for exact solutions, which are constructed for the 2D case below. It also has applications to real systems, such as bacterial colony growth [14], where the square-gradient term corresponds to nonlocal growth occurring at concentration gradients. The square-gradient term is also similar to the nonlinear terms in the Kuramoto–Sivashinsky equation for propagating flame (where it appears as a consequence of the curvature of the flame front) [15] and in the theory of growing interfaces [16].

When $m = 2$, the transformation $\phi = 1 - v^{-1}$ converts equation (1) into $v_t - \Delta v = v - 1$, and further, in terms of $w = v - 1$, into the linear diffusion (heat) equation [17]

$$w_t - \Delta w = w \tag{2}$$

solutions for which, and therefore for equation (1) ($\phi = 1 - \frac{1}{1+w}$), can be completely characterized. It is natural to approach the analysis of the system in two steps: first to identify stationary configurations—the spectrum of states the system evolves to, and then to solve the initial value (Cauchy) problem and thereby to partition the space of initial states into basins of attractions for finite configurations. We address here only the first step, leaving the second one for future consideration.

2. Travelling waves in one spatial dimension

Galilean invariance of equation (1) provides solutions propagating along a certain direction with constant speed (travelling waves). In one dimension, equation (1) reduces for travelling waves to

$$-c\phi' - \phi'' - \frac{m}{1-\phi}(\phi')^2 = \phi(1-\phi) \tag{3}$$

where a prime denotes the derivative with respect to the moving coordinate frame, $\xi = x - ct$, with c being the velocity of the wave.

Fisher found [18] that equation (3), with $m = 0$, has an infinite number of travelling wave solutions for which $0 \leqslant \phi(x,0) \leqslant 1$ and wave speeds are $c \geqslant c_{\min} = 2$. Kolmogorov *et al* [19] proved that for bounded $\phi(x,0)$, if $\phi(x,0) = 1$ for $x < a$, and $\phi(x,0) = 0$ for $x > b$, there is a unique solution of (3), with $m = 0$, and that this solution evolves into a monotonic travelling wave solution (kink-like, $\phi(x \to -\infty) \to 1$, $\phi(x \to +\infty) \to 0$) with a speed $c = c_{\min}$. Higher velocity waves arise when an appropriate initial gradient is present in the system: the less steep the wave profile, the faster it moves [20]. McKean [21] showed that any wave speed $c > 2$ is stable (with respect to small perturbations) if the initial datum has the right behaviour at the tails. A travelling wave solution for (3), with $m = 0$, in explicit form, was found by Ablowitz and Zeppetella [22] for one special case:

$$\phi(x,t) = [1 + \exp(\xi/\sqrt{6})]^{-2}. \tag{4}$$

The kink (4) propagates from, say, left to right with a speed $c = 5/\sqrt{6} \approx 2.041$. The problem of selection of appropriate speed has been discussed in [20, 23, 24]. Fronts initiated on a compact support evolve to minimum velocity solutions [23]. Travelling wave solutions for (3), with $m = 0$ and $c < 2$, also exist but they are considered to be physically unrealistic since ϕ becomes negative for some ξ: $\phi \to 0$ at the leading edge with decreasing oscillations around $\phi = 0$.

Travelling waves for the 1D equation (3), with $m = 2$, were studied in [17]. The general solution for equation (2) can be expressed as the linear superposition of modes

$$\tilde{w}(\omega) = \exp\left(\pm\sqrt{\omega - 1}x + \omega t\right) \tag{5}$$

with weights determined by initial conditions†. The modes decay rapidly when $\omega < 0$ and are periodic in space if $\omega < 1$. We are interested in the case of travelling waves, $\omega > 1$. The single-mode, travelling wave solution propagating from left to right reads then

$$\phi(x,t) = 1 - \frac{1}{1 + A\exp\left[-\sqrt{\omega-1}(x-ct)\right]} = \left[1 + A^{-1}\exp\left(\sqrt{\omega-1}\xi\right)\right]^{-1} \tag{7}$$

where A is (here and further) some positive constant, and the velocity of the wave is uniquely defined by its slope via

$$c = \frac{\omega}{\sqrt{\omega-1}}. \tag{8}$$

The function $c(\omega) > 0$ has a 'check-sign' shape, with a minimum at $c = 2$ when $\omega = 2$. Therefore, two waves can, except for the minimal case, propagate with the same velocity c: a sharp wave with slope $\sqrt{\omega-1} = \frac{c+\sqrt{c^2-4}}{2}$, and a shallow wave, for which $\sqrt{\omega-1} = \frac{c-\sqrt{c^2-4}}{2}$. The shallow wave coincides in the limit $\omega \to 1$ with the approximate solution for the classic Fisher equation, the solution obtained by neglecting the second derivative in equation (3) when $m = 0$.

On the other hand, selection of a value for ω uniquely defines the velocity of the wave. One can show, by direct integration of equation (2), that initial perturbations generated on compact supports (or even those which just do not have an infinite tail, e.g. step function) develop into the travelling wave of minimal velocity.

3. Travelling waves in two spatial dimensions

In a 2D medium wave propagation is more complicated because of a multiplicity of travelling waves. We assume here that, after an initial relaxation process, a wavefront propagates along a certain direction with constant velocity and invariable shape‡. Such stationary propagating waves are known for a variety of nonlinear wave models, e.g. 2D Korteveg–de Vries (KdV) waves [25], the sine–Gordon equation [26, 27] and excitable media [28]. The patterns are building blocks for constructing possible stationary wave configurations in a layered medium [29], e.g., stationary refracting and reflecting waves [30]. Approximate travelling wave solutions with nontrivial fronts have been recently constructed for the quadratic Fisher equation [7] (equation (1) with $m = 0$). The complete integrability of equation (1) for $m = 2$ allows us to study for the first time the multiplicity of dissipative waves on the basis of exact solutions.

For the case, $m = 2$ in two dimensions, we solve

$$w_t - w_{xx} - w_{yy} = w \tag{9}$$

by the method of separation of variables

$$w(t,x,y) = T(t)\cdot X(x)\cdot Y(y). \tag{10}$$

This generates three independent linear equations of the form

$$T' - \omega T = 0 \tag{11a}$$

$$X'' - (\omega - 1 - \lambda)X = 0 \tag{11b}$$

$$Y'' - \lambda Y = 0 \tag{11c}$$

† The linear superposition rule valid for solutions of equation (2) leads to the following nonlinear superposition rule for the solution of the initial equation (1):

$$\frac{\phi_3}{1-\phi_3} = \frac{\phi_1}{1-\phi_1} + \frac{\phi_2}{1-\phi_2}. \tag{6}$$

‡ Rigidly rotating, spiral-like solutions observed in excitable media are not possible in a 'Fisher-like' medium because its elements, in contrast to an excitable medium, do not return to their initial state after the passage of the wave.

with ω and λ being separation constants. As in the 1D case, ω is chosen here to be positive, and when $\lambda = 0$, equations (11*a*), (11*b*) coincide with equivalent equations for the 1D case. In general, solutions for equations (11*a*)–(11*c*) are combinations of exponential functions

$$T(t) = T_0 \exp(\omega t) \tag{12a}$$

$$X(x) = X_1 \exp\left(-\sqrt{\omega - 1 - \lambda}x\right) + X_2 \exp\left(\sqrt{\omega - 1 - \lambda}x\right) \tag{12b}$$

$$Y(y) = Y_1 \exp(-\sqrt{\lambda}y) + Y_2 \exp(\sqrt{\lambda}y) \tag{12c}$$

with T_0, $X_{1,2}$, $Y_{1,2}$ being integration constants. There are two special cases: (i) $\omega - 1 - \lambda = 0$, when

$$X(x) = X_3 \cdot x + X_4 \tag{13}$$

and (ii) $\lambda = 0$, when

$$Y(y) = Y_3 \cdot y + Y_4. \tag{14}$$

Here $X_{3,4}$, $Y_{3,4}$ are again integration constants.

We are looking for wave-like solutions that travel along the x axis, so x and t must enter the solution in a linear combination, $x - ct$, which is impossible with (13). Thus we write $w(t, x, y)$ in the form

$$w = \left[X_1 \exp\left(-\sqrt{\omega - 1 - \lambda}x + \omega t\right) + X_2 \exp\left(\sqrt{\omega - 1 - \lambda}x + \omega t\right)\right] Y(y) \tag{15}$$

with $Y(y)$ given by either (12*c*) or (14). Also, to avoid solutions that oscillate in the X direction, we restrict λ to the half-line $\omega - 1 > \lambda$. The two bracketed terms in (15) correspond to waves travelling in opposite directions. Restricting ourselves to waves propagating in the positive direction of the x axis, we write

$$w(t, x, y) = w(\xi = x - V_p t, y) = X_1 \exp\left(-\sqrt{\omega - 1 - \lambda}\xi\right) Y(y) \tag{16}$$

where the wave propagation velocity is connected to ω and λ via

$$V_p = \frac{\omega}{\sqrt{\omega - 1 - \lambda}}. \tag{17}$$

Using (8), we can also express V_p as a function of plane-front velocity, c. Depending on the sign and magnitude of λ, we may expect patterns moving slower or faster than a plane wave.

3.1. *Plane waves*

The trivial generalization of 1D solutions for the 2D case is a plane wave propagating with velocity $V_p = c$ along the x axis ($\lambda = 0$, $Y_3 = 0$). The front line (a line of a constant level, $\phi = \text{const}$) is a straight line perpendicular to the x axis. This travelling wave connects homogeneous asymptotic states $\phi(\xi \to -\infty, y) = 1$ and $\phi(\xi \to \infty, y) = 0$.

The simplest travelling wave solutions involving both x and y space variables can be constructed from the plane wave by rotating the frame of reference†. For instance, a plane wave propagating with velocity c in the direction at an angle $\pm\varphi$ from the x axis is given by

$$\phi(x, y, t) = 1 - \frac{1}{1 + A \exp\left[-\sqrt{\omega - 1}(x \sin\varphi \mp y \cos\varphi) + \omega t\right]}. \tag{18}$$

Equivalently, the wave can be thought of as a tilted plane wave propagating along the x axis

$$\phi(x, y, t) = 1 - \frac{1}{1 + A \exp\left[-\sqrt{\omega - 1} \sin\varphi(x - V_p t) \pm \sqrt{\omega - 1} y \cos\varphi\right]} \tag{19}$$

† Note that this simple idea does not necessarily work for any nonlinear wave model. It works for the sine–Gordon equation but fails when applied to certain 2D extensions of KdV or Burger equations.

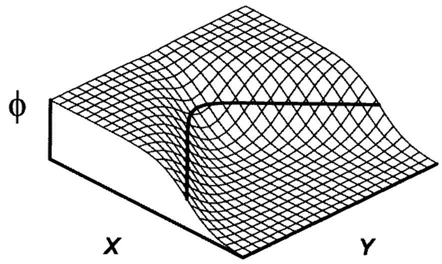

Figure 1. V-shaped wave. Here $\omega = 2$ as for the minimal wave, and $\lambda = \frac{1}{2}$, which corresponds, according to (22), to $\alpha = \pi/2$ = angle between wings of the V wave. The thick solid curve shows the level line $\phi_l = 0.5$.

with velocity

$$V_p = c/\sin\varphi. \tag{20}$$

On the other hand, the corresponding expression constructed from (16), (12*c*) reads

$$\phi(\xi, y) = 1 - \frac{1}{1 + A\exp\left[-\sqrt{\omega - 1 - \lambda}\xi \pm \sqrt{\lambda} y\right]}. \tag{21}$$

Comparing (19), (21) we get a relationship between λ and φ:

$$\sqrt{\lambda} = \sqrt{\omega - 1}\cos\varphi. \tag{22}$$

Since for the wave with a positive velocity component along the x axis φ runs from 0 to $\pm\pi/2$, equation (22) restricts λ to the segment

$$0 \leqslant \lambda \leqslant \omega - 1. \tag{23}$$

3.2. V waves

If we look for solutions invariant to inversion of y, we must restrict $Y(y)$ to be an even function. The choice $Y_1 = Y_2$ in (12*c*) leads then, for λ from the segment (23), to

$$\phi(\xi, y) = 1 - \frac{1}{1 + A\exp\left(-\sqrt{\omega - 1 - \lambda}\xi\right)\cosh(\sqrt{\lambda} y)}. \tag{24}$$

This is the so-called V pattern (figure 1), known for Fisher's equation [7] and in excitable media [28]. The front consists of two extended, almost flat wings colliding at a certain asymptotic angle α. In the point of collision, the wings are connected with each other by a smooth curved area ($\sim\lambda^{-1/2}$) where the front line turns rapidly. Like the plane wave, a V pattern connects homogeneous asymptotic states. The connection of the separation constant λ to the asymptotic angle α between wings of the V wave can be found easily because, for large $|y|$, the wings of the V wave are plane waves tilted at angles $\pm\varphi_\infty$ (i.e., $\alpha = 2\varphi_\infty$). Hence $\sqrt{\lambda} = \sqrt{\omega - 1}\cos\varphi_{\pm\infty}$.

A V wave is a tachyonic solution, i.e., it propagates faster than a plane wave. It is also interesting to mention that solution (24) coincides with an approximate solution for the V wave of the quadratic Fisher equation (equation (1) with $m = 0$) we have constructed earlier [7].

3.3. Oscillatory solutions

If now $\lambda < 0$, the real function $Y(y)$ in (12*c*) turns into the trigonometric cosine, leading therefore to the front oscillating in space:

$$\phi(\xi, y) = 1 - \frac{1}{1 + A\exp\left(-\sqrt{\omega - 1 - \lambda}\xi\right)\cos\left(\sqrt{-\lambda} y\right)}. \tag{25}$$

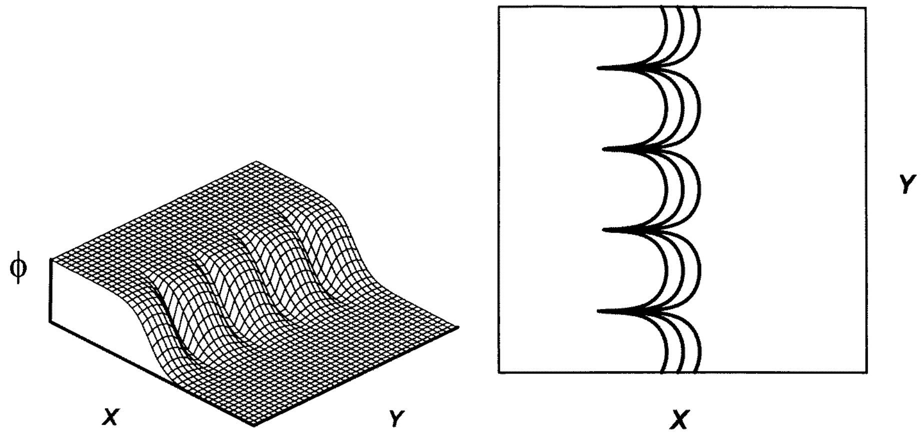

Figure 2. Space oscillating front (propagating fingers) for $\omega = 2$, and $\lambda = -\frac{1}{2}$: (*a*) surface plot; (*b*) three curves of constant level: $\phi_l = 0.25$, 0.5 and 0.75.

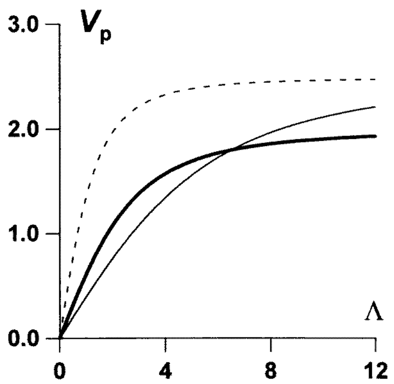

Figure 3. Dispersion curves for the space oscillating solutions: the thick solid curve is for $c = 2$, while the thin solid and dashed curves are for $c = 2.5$, for shallow and sharp waves respectively.

This solution is singular because the denominator in expression (25) becomes zero for some value of ξ and y. However, not only is $Y(y) \sim \cos(\sqrt{-\lambda}y)$ a solution of (11*c*) but so also is $Y(y) \sim |\cos(\sqrt{-\lambda}y)|$. Using the latter solution we can construct bounded space-oscillating fronts in the form

$$\phi(\xi, y) = 1 - \frac{1}{1 + A\exp\left(-\sqrt{\omega - 1 - \lambda}\xi\right)\left|\cos\left(\sqrt{-\lambda}y\right)\right|}. \tag{26}$$

A typical pattern of these propagating 'fingers' is shown in figure 2. The wavelength of the front, $\Lambda = \pi/\sqrt{-\lambda}$, runs from π, when $\lambda = -1$, to ∞ (the front converts into a plane wave), when $\lambda \to 0$. As $\lambda \to -\infty$, the wavelength of the pattern drops to zero. Using (17), we can write the 'dispersion' relationship (the dependence of wave speed on the wavelength):

$$V_p = \frac{c}{\sqrt{1 + \frac{1}{\omega - 1}\left(\frac{\pi}{\Lambda}\right)^2}}. \tag{27}$$

Several different curves are depicted in figure 3. Qualitatively they are similar to those found for Fisher's equation in [7].

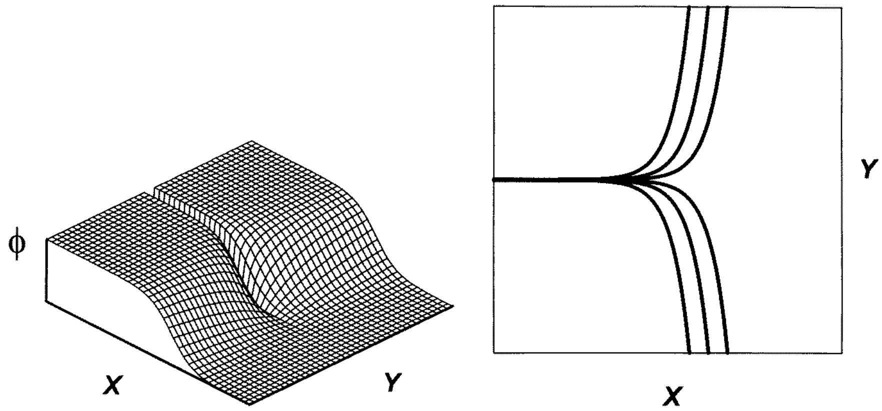

Figure 4. Separatrix solution ($\omega = 2$): (*a*) surface plot; (*b*) three curves of constant level: $\phi_l = 0.25$, 0.5 and 0.75.

3.4. Separatrix

The case $\lambda = 0$, $Y_3 = 0$ describes, as we discussed earlier, a plane wave moving along the x axis with velocity $V_p = c$. If $Y_3 \neq 0$ but $Y_4 = 0$, we get an inhomogeneous solution of the form

$$\phi(x,t) = 1 - \frac{1}{1 + A|y| \exp\left(-\sqrt{\omega - 1}\xi\right)}. \tag{28}$$

This 'separatrix' solution and level lines ($\phi = \phi_l \equiv$ const) are depicted in figure 4. The level lines straighten out, as $y \to \pm\infty$, and become orthogonal to the x axis. Therefore, they propagate with the velocity of a plane wave ($V_p = c$). Thus, in 2D unrestricted media there exist two waves, the plane wave and the separatrix wave, which propagate with speed c.

3.5. Y waves

One more option exists for positive λ:

$$\phi(\xi, y) = 1 - \frac{1}{1 + A \exp\left(-\sqrt{\omega - 1 - \lambda}\xi\right) |\sinh(\sqrt{\lambda} y)|}. \tag{29}$$

This solution, known as a 'Y wave', differs qualitatively from the separatrix solution only by the angle between asymptotes $2\varphi_\infty$: for the former it can be any positive value between zero and π, while for the latter it is exactly π. The connection between λ and φ_∞ is identical to the one for V waves.

4. Velocity-curvature dependence

For systems with dissipative loss supporting propagating waves, a low-level model can often be formulated to simplify the description of solitary waves, which in the 2D case approximates the propagating wavefront with an evolving front line [26,31–35]. The crucial concept connecting such geometric models to their microscopical (PDE) counterparts is the dependence of local wave velocity, V, of the wave on the curvature of the front line, k. (Therefore, models of this kind are sometimes referred to as curvature-driven interface models.) $V(k)$ is a linear function (for $|k|$ small) for crystal growth problems [31, 35] and for excitable media (eikonal approximation) [36]. For excitable media, $V(k)$ remains almost a linear function for negative k but deviates from the eikonal approximation significantly for positive k, exhibiting a critical value beyond which stationary propagation of the curved front is impossible. Experiments with waves in a chemical excitable medium (the Belousov–Zhabotinsky reaction) confirm qualitatively such behaviour [37]. Recently, a nonlinear, cubic-like curve, $k = k(V)$ has been derived for the stationary propagating fronts of Fisher's equation on the basis of approximate 2D solutions [7]. Theoretical derivations of $V(k)$ are usually based on semi-phenomenological arguments or on perturbation analysis of corresponding PDE models. The solutions we have found in section 2 allow us, for the first, time to construct exact analytical expressions for $V(k)$ from nontrivial solutions of a 2D reaction–diffusion-like PDE model.

We associate a front line with a line of constant level $\phi(\xi, y) = \phi_l = \text{const}$. This defines a curve in the plane (ξ, y). The curvature of the front line is then given by $k = \frac{\mathrm{d}^2 y/\mathrm{d}\xi^2}{[1+(\mathrm{d}y/\mathrm{d}\xi)^2]^{3/2}}$. Furthermore, the velocity of stationary patterns propagating along the x axis is related to the local normal velocity of the front line as $V = V_p \sin\varphi$, where the angle between the x axis and the tangent to the front line, φ, can be evaluated from the relationship $\frac{\mathrm{d}y}{\mathrm{d}\xi} = -(\frac{\phi_\xi}{\phi_y})_{\phi=\text{const}} = \tan\varphi$. Appropriately combining these three expression we may find $V(k; \phi_l)$.

The dependence of the normal velocity on front curvature determined for V (24) and Y waves (29), space-oscillating (25), and separatrix (28) waves in the above-described way turns out, remarkably, to be the same expression:

$$k = \gamma \left[1 - \left(\frac{V}{c}\right)^2\right] \left(\frac{V}{c}\right) \tag{30}$$

where

$$\gamma = \sqrt{\omega - 1}\left(1 - \frac{\lambda}{\omega - 1}\right). \tag{31}$$

This relationship is independent of the level line chosen because, as can be seen from the general solution, all lines of constant level have, for a given pattern, the same shape. For a plane wave, $k = 0$, $\lambda = 0$ and $V = c$. $\lambda = 0$ also for the separatrix solution. For other waves, λ can be replaced by a meaningful, pattern-dependent parameter: for the V- and Y-shaped waves, λ is a function of the asymptotic angle, $\lambda = (\omega - 1)(\sin\varphi_\infty)^2$, while for the oscillating front λ is related to the wavelength of the pattern, $\Lambda = \pi/\sqrt{-\lambda}$.

The cubic-like curve (30) is depicted in figure 5. The similar antisymmetric branch for negative V is not shown in the figure. The portion of the curve which starts from zero and

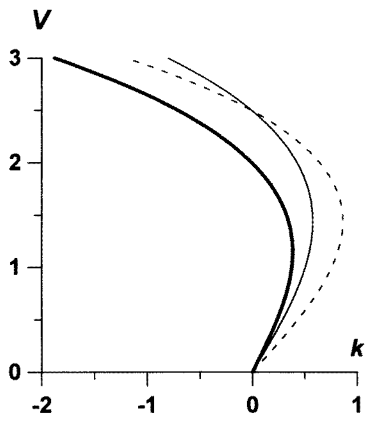

Figure 5. Dependence of the local normal front velocity on front curvature. The thick solid curve corresponds to the separatrix case, $\lambda = 0$, with $\omega = 2$, hence, $\gamma = 1$. The thin solid and dashed curves are for $c = 2.5$ and $\lambda = -\frac{1}{2}$ (space oscillating solution) for shallow ($\omega = 1.25$, $\gamma = 1.5$) and sharp ($\omega = 5$, $\gamma = 2.25$) waves respectively.

has positive inclination is usually associated with nonstable waves; the rest of the curve has negative slope, reflecting the stabilizing role of diffusion [38]. The maximum positive curvature $k_{cr} = \frac{2\gamma}{3\sqrt{3}}$ achievable on a stationary propagating front depends on spatial characteristics of the pattern, because γ depends on λ. The fragment of the front with the maximum curvature moves with the slowest velocity $V_{cr} = c/\sqrt{3}$, which, surprisingly, is independent of λ.

For small curvatures (30) becomes

$$V = c - \frac{c}{2\gamma}k. \tag{32}$$

For the wave of minimal speed, $c = c_{\min} = 2$, equation (32) recovers the eikonal approximation for excitable media (with the coefficient in front of k equal to unity) if we take into account the fact that small curvature can be realized only if λ is small (e.g., V waves with large asymptotic angle, therefore close to plane wave, or oscillating fronts with large periods). For large negative curvature, equation (30) gives the deviation of V from the linear approximation (32) towards smaller V. Also notice that equation (30) turned out to be identical to the V of k dependence derived for travelling waves in Fisher's equation [7].

5. Static structures

Static structures appear as a special case for travelling waves when $V_p = 0$. In one dimension, the static equation (2) is a single-mode harmonic oscillator, implying that

$$\phi(x) = 1 - \frac{1}{1 + w_0|\cos(x)|} \tag{33}$$

with w_0 being (here and throughout) a positive integration constant. By contrast, the 2D static case, described by equations (11*b*), (11*c*) with $\omega = 0$, admits multiple frequencies for either X or Y. Thus, the additional spatial degree of freedom introduces a one-parameter family of static solutions (parametrized by λ).

We consider only the region $\lambda \leqslant -\frac{1}{2}$, since the complementary case $\lambda > -\frac{1}{2}$ can be obtained from the first one by interchanging x and y. General static solutions are then combinations of exponential functions (12*b*), (12*c*) except for the special case, this time at $\lambda = -1$, when $X(x)$ turns into a first-order polynomial (13). For negative λ, equation (12*c*) takes the form

$$Y = Y_0 \cos\left(\sqrt{-\lambda}y\right) \tag{34a}$$

with Y_0 being an integration constant.

The trivial generalization of 1D periodic static structures to two dimensions corresponds to the special case $\lambda = -1$ with $X_3 = 0$. The corresponding family of solutions $\phi(x, y) = \phi(y)$ (parametrized, e.g., by X_4) repeats the behaviour of 1D solutions in the Y direction and remains homogeneous (invariable) in the X direction. The pattern of parallel stripes has a unique period π, but variable amplitude and flatness of the humps determined by X_4.

For $-1 \leqslant \lambda < -\frac{1}{2}$, solutions for both X and Y are trigonometric functions, giving

$$\phi(x, y) = 1 - \frac{1}{1 + w_0\left|\cos\left(\sqrt{1+\lambda}x\right)\right|\left|\cos\left(\sqrt{-\lambda}y\right)\right|}. \tag{34b}$$

When $\lambda = -\frac{1}{2}$, the spatial periods are equal in both directions, producing the 'chicken skin' pattern depicted in figure 6. The spatial period in this case ($\lambda = -\frac{1}{2}$) is $\sqrt{2}$ times larger than the spacing of the stripes in the previous case ($\lambda = -1$). As λ decreases, the humps elongate

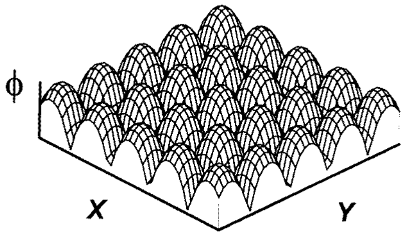

Figure 6. 2D static solutions for $\lambda = -\frac{1}{2}$: 'chicken skin' pattern.

in X and shrink in Y directions. Notice also that, when boundary conditions are applied, these structures require a minimal system size for their existence.

Standing finger patterns, similar in shape to the moving ones, appear when $\lambda < -1$ and one of the integration constants, X_1 or X_2, is zero. Then

$$\phi(x, y) = 1 - \frac{1}{1 + w_0 \exp\left[\pm\sqrt{-1-\lambda}x\right]\left|\cos\left(\sqrt{-\lambda}y\right)\right|}. \tag{34c}$$

In order to consider only the bounded solution, we assume that $w_0 > 0$, and take the absolute value of the cosine. Notice that, as λ decreases, the spatial period in the Y direction decreases and the kink in the X direction becomes steeper.

Several other static structure are possible when $X(x)$ is chosen to be $\cosh(\sqrt{-1-\lambda}x)$, $|\sinh(\sqrt{-1-\lambda}x)|$ or $|x|$. Qualitatively, these structure look like two sets of standing finger patterns pointing at each other across the y axis. Standing vortexes, such as those known for the sine–Gordon equation [39], are not possible in our case because, for any λ, at least one component, $X(x)$ or $Y(y)$, is a space-oscillating function.

Static structures with circular symmetry can also be constructed by separation of variables, $w = R(r)\Phi(\varphi)$. The radial component $R(r)$ then turns out to be a Bessel function $J_n(r)$ and the angular component $\Phi(\varphi)$ is a trigonometric function. Therefore, single-mode solutions for ϕ are given by

$$\phi(r) = 1 - \frac{1}{1 + w_0 J_n(r)\cos(n\varphi)} \tag{35}$$

where $0 < w_0 < 1$ (to eliminate singular solutions), and we have omitted a phase-shifting constant. The case $n = 0$ corresponds to a 'Mexican hat' isotropic solution, while $n > 0$ leads to solutions with broken symmetry.

6. Discussion and conclusions

Our investigation shows explicitly that stationary travelling waves in a 2D reaction–diffusion-like system may have different geometries, which, together with the reaction rate and diffusion coefficient, affects the propagation velocity of waves. In an unbounded, spatially homogeneous medium, five characteristic solutions have been identified: plane, V, and Y waves, a 'separatrix' wave, and space-oscillating propagating fronts. The possibility of time-invariant propagating fronts with such geometries was predicted in [40] on the basis of a coarse-scale geometrical model. This work constitutes the first constructive proof of the existence of these waves. When the medium becomes bounded (an infinitely long stripe) and no flux is allowed through the boundaries, only two waves survive (plane and oscillating), because the front line of the wave must approach the boundary orthogonally.

The velocity of the wave V_p may be considered as a bifurcation parameter. The slowest wave is an oscillating front; its velocity increases with increasing wavelength. When velocity reaches the value corresponding to the plane wave, c, the wavefront bifurcates into two distinct configurations, a plane wave and a 'separatrix' wave, which give birth with an increase of V_p to V and Y waves, respectively. The Cauchy problem for equation (1), answering the question of which initial conditions lead to which stationary travelling waves, remains to be explored.

Fisher's equation is a prototype for nonlinear models of many different sorts. Therefore its solutions are reminiscent of patterns seen in different fields. V waves have been characterized in crystal-growth models [35] and in excitable media [28], but only in the framework of geometrical (kinematic) models. Space-oscillating fronts are reminiscent of solidification fingers [41], and may be relevant to cellular flame structures and patterns arising from diffusion-induced instability of the planar front in chemical reaction–diffusion systems [42]. The solutions we have constructed may be good starting points for developing more elaborate PDE-based theories of these patterns.

Media capable of supporting periodic trains of plane waves, e.g. excitable media, exhibit often a dependence of wave velocity on the spacing μ between pulses, which is traditionally called the 'dispersion relationship' . Media described by Fisher-type equations are not able to support periodic wave trains, but, as we have shown, in two dimensions they support isolated travelling waves with space-oscillating fronts (the hump-like front fragment repeats itself in the direction orthogonal to its direction of propagation). Such waves exhibit a nontrivial dependence of front velocity on spatial period (wavelength) Λ (see also [7]). This kind of the dispersion relation is different in its underlying mechanism because dispersion in excitable media is due to the influence of a second component, an 'inhibitor' , which is absent in our case. Nevertheless, the dispersion curve we have constructed is qualitatively similar to the one found in 1D excitable media.

The velocity-curvature dependence we found exhibits a critical curvature, similar to the case of excitable media [36]. In excitable media the critical curvature is thought to be attributable to the presence of an inhibitor in the system, but our study shows that critical curvature is present even in a scalar model. In excitable media a front whose curvature exceeds the critical curvature breaks at this point and may evolve consequently into spirals. The scenario for the evolution of supercritical fronts in Fisher-like systems is not clear yet.

Acknowledgments

This work was supported by NSF Grants DMS-9525766 and CHE-9500763.

References

[1] Novikov S, Manakov S V, Pitaevskii L P and Zakharov V E 1984 *Theory of Solitons. The Inverse Scattering Method* (New York: Consultants Bureau)

[2] Hirota R 1972 *J. Phys. Soc. Japan* **33** 1456

[3] Lamb G L Jr 1971 *Rev. Mod. Phys.* **43** 99
Leibbrandt G 1976 *Phys. Rev.* B **15** 3353

[4] Infeld E and Rowlands G 1990 *Nonlinear Waves, Solitons and Chaos* (Cambridge: Cambridge University Press)

[5] Gardner R 1986 *J. Diff. Eqns* **61** 335
Gardner R 1986 *Lect. Appl. Math.* **23** 383

[6] Puri S, Elder K R and Desai R C 1989 *Phys. Lett.* A **142** 357
Keener J P 1986 *SIAM J. Appl. Math.* **46** 1039

[7] Brazhnik P K and Tyson J J 1998 *SIAM J. Appl. Math.* accepted for publication

[8] Frank-Kamenetskii D A 1955 *Diffusion and Heat Exchange in Chemical Kinetics* (Princeton, NJ: Princeton University Press)
Williams F A 1965 *Combustion Theory* (Reading, MA: Addison-Wesley)

[9] Murray J D 1977 *Lectures on Nonlinear-Differential-Equations Models in Biology* (London: Oxford University Press)
Britton N F 1986 *Reaction–Diffusion Equations and their Applications to Biology* (London: Academic)
[10] Tuckwell H C 1988 *Introduction to Theoretical Neurobiology (Cambridge Studies in Mathematical Biology)* (Cambridge: Cambridge University Press) p 8
[11] Cohen H 1977 *Nonlinear Diffusion Problems (Studies in Applied Mathematics)* ed A H Taut (Englewood Cliffs, NJ: Prentice-Hall)
Fife P C and McLeod J B 1977 *Arch. Ration. Mech. Anal.* **65** 335
Aronson D G and Weinberger H F 1975 *Nonlinear Diffusion in Population Genetics, Combustion and Nerve Pulse Propagation (Lecture Notes in Mathematics)* ed J A Goldstein (New York: Springer) p 446
[12] Bramson M D 1978 *Comment. Pure Appl. Math.* **31** 531
[13] Canosa J 1969 *J. Math. Phys.* **10** 1862
[14] Grimson M J and Barker G C 1994 *Phys. Rev.* E **56** 1680
[15] Margolis S B and Matkowsky B J 1983 *Combust. Sci. Technol.* **34** 45
[16] Kardar M, Parisi G and Zhang Y-C 1986 *Phys. Rev. Lett.* **56** 889
[17] Wang X Y, Fan S and Kyu T 1997 *Phys. Rev.* E **56** R4931
[18] Fisher R A 1937 *Ann. Eugen.* **7** 355
[19] Kolmogorov A N, Petrovsky I G and Piskunov N S 1988 Study of the diffusion equation with growth of the quantity of matter and its application to a biology problem *Dynamics of Curved Fronts* ed P Pelcé (New York: Academic) p 105
[20] Murray J D 1989 *Mathematical Biology* (Berlin: Springer)
[21] McKean H P 1970 *Adv. Math.* **4** 209
[22] Ablowitz M J and Zeppetella A 1979 *Bull. Math. Biol.* **41** 835
[23] Merkin J H and Needham D J 1989 *J. Eng. Math.* **23** 343
[24] Gray P, Merkin J H, Needham D J and Scott S K 1990 *Proc. R. Soc.* A **430** 509
[25] Segur H 1986 *Physica* D **18** 1
[26] Malomed B A 1991 *Physica* D **52** 157
[27] Vitanov N K 1996 *J. Phys. A: Math. Gen.* **29** 5195
[28] Brazhnik P K and Davydov V A 1995 *Phys. Lett.* A **199** 40
[29] Brazhnik P K and Tyson J J 1997 *Physica* D **102** 300
[30] Brazhnik P K and Tyson J J 1996 *Phys. Rev.* E **54** 1958
[31] Burton W K, Cabrera N and Frank F C 1951 *Phil. Trans. R. Soc.* A **243** 299
[32] Whitham E 1974 *Linear and Nonlinear Waves* (New York: Wiley)
[33] Brazhnik P K, Davydov V A and Mikhailov A S 1988 *Theor. Math. Phys.* **74** 300
[34] Davydov V A, Zykov V S and Mikhailov A S 1994 *Physica* D **70** 1
[35] Schwendeman D W 1996 *SIAM J. Appl. Math.* **56** 1523
[36] Zykov V S 1987 *Simulation of Wave Processes in Excitable Media* ed A T Winfree (Manchester: Manchester University Press)
[37] Nagy-Ungvarai Z, Ungvarai J, Muller S C and Hess B 1992 *J. Chem. Phys.* **97** 1004
[38] Mikhailov A S 1990 *Foundations of Synergetics. I. Distributed Active Systems* (Berlin: Springer)
[39] Hudak O 1982 *Phys. Lett.* A **89** 245
[40] Brazhnik P K 1996 *Physica* D **94** 205
[41] Pelcé P 1988 *Dynamics of Curved Fronts* (New York: Academic)
[42] Scott S K and Showalter K 1992 *J. Chem. Phys.* **96** 8702
Showalter K 1995 *Nonlinear Sci. Today* **4** 1